Optimization of welded K-node in offshore jacket structure including the stochastic size effect

Mikkel Løvenskjold Larsen [a], Vikas Arora [a,*], Sondipon Adhikari [b], Henrik Bisgaard Clausen [c]

[a] *Department of Mechanical and Electrical Engineering, University of Southern Denmark, Campusvej 55, 5530, Odense, Denmark*
[b] *James Watt School of Engineering, The University of Glasgow, Glasgow, UK*
[c] *Ramboll Energy, Denmark*

A B S T R A C T

Offshore structures are exposed to cyclic loading and thereby at risk of fatigue failure, especially at the welded joints between trusses in offshore jacket foundations. In this paper, an optimization framework for welded joints considering fatigue damages is presented. The framework can be used to optimize the orientation and location of welds connecting the joint in a welded K-node in offshore jacket structures considering fatigue damage. It is known that longer welds are at higher risk of fatigue failure compared to shorter welds. To account for this, the statistical size effect is modelled using the Karhunen-Loéve expansion which can be used to take into account the effect of longer welds in the damage assessment. The approach is included in the optimization framework and it is shown that using this method it is possible to simulate the effect of having a good welding quality and a poor welding quality using the correlation length and coefficient of variation. The proposed optimization framework is validated on a simple plate structure and the effect of the statistical input parameters in the statistical size effect is examined. The results show that the proposed optimization approach is robust in predicting the expected tendencies for a simple plate structure. Furthermore, a full-scale welded K-node in an offshore jacket structure manufactured using cast steel is optimized with respect to mass. The optimization is performed considering a good quality weld and a poor-quality weld by including the statistical size effect. The results show that using high quality welds will result in lower mass of the K-node.

1. Introduction

Offshore welded jacket structures are exposed to cyclic wind and wave loadings and are prone to fatigue damage. The welded joints between the tubulars (called nodes) are of special interest because these joints are highly loaded, the geometry of the joints leads to stress raisers and welds include possible defects resulting in premature crack initiation [1]. New possibilities for manufacturing welded joints using casting allows for more fatigue efficient structures [2,3]. An example of a traditional welded offshore node is shown in Fig. 1, together with an alternative version which can be made using cast steel.

As seen from Fig. 1, the traditional hollow-section joint can be replaced with a cast section, which allows for a more fatigue effective design by moving the welds away from the high-stress areas and by fabricating smoother transitions between the braces (smaller pipes)

---

and chord (large pipe). However, finding the optimum design of these new fatigue efficient cast joints is a complex task.

Optimization of structures considering fatigue damage has been investigated rigorously in the last two decades [4–8]. These investigations include size optimization, shape optimization and topology optimization considering different types of structures and fatigue criteria. Thus, much effort has been made in the field of structural optimization considering fatigue constraints, however, two main issues are rarely addressed.

Firstly, the fatigue criterion used to predict the fatigue damage is rarely consistent, when using different guidelines. Often, the fatigue analysis of offshore structures is based on the S–N curve (or Wöhler curve) approach [9]. This approach is well described in governing standards and guidelines by the IIW [10], DNV [11] and the Eurocode [12]. However, the damage criteria for which the stresses in the structure are to be combined with the relevant S–N curves vary between the different guidelines. Furthermore, the codes and guidelines are subjected to updates over time. This makes it difficult to develop a general optimization software that is valid for multiple different fatigue criteria, which require additional sensitivity analyses of the fatigue constraints. Thus, a generalized optimization framework, which can easily be adapted for other fatigue criteria is required.

Secondly, the fatigue lives of welded joints are highly uncertain [13]. When the length and size of the welds are altered during the optimization procedure, the probability of failure varies. This can be attributed to various causes, one of the influencing factors is the so-called thickness effect or size effect [10–12]. The size effect describes how the fatigue life will decrease with increasing wall thickness and weld volume. The size effect is often assumed to be influenced by three overall effects, namely: the geometric size effect, the technological size effect and the statistical size effect [14]. The statistical size effect can be explained by the fact that a higher risk of failure is present with more welding material. The statistical size effect is governed by the weld length rather than the thickness [14, 15]. To account for this effect, expressions for calculating the reduced fatigue life due to thickness and length of the welds are included in the governing guidelines [10–12]. However, in these governing guidelines, deterministic approaches are used.

In recent times, the stochastic finite element method (SFEM) has become an increasingly used approach for incorporating randomness and uncertainty quantification in structural responses [16–18]. SFEM has been used in many applications for uncertainty quantification, as summarized in the review paper by Arregui-Mena et al. [19]. Some research efforts have been carried out to use SFEM for fatigue analysis of structures [20,21]. Recently, Larsen et al. [22], investigated the effect of randomness in hot-spot stress extrapolation points for fatigue analysis of two full-scale offshore K-node structures. The results showed that misplacement of extrapolation points highly influenced the predicted fatigue lives of the K-nodes. Thus, the effect of randomness in the fatigue analysis of offshore K-node structures should be taken into account.

In this paper, a new generalized optimization framework for welded joints in offshore jacket structures have been developed with focus on easy implementation of different fatigue criteria and considering the stochastic size effect. The developed framework can be used to optimize any structure based on the fatigue damages or fatigue lives considering the stochastic size effect. Firstly, the optimization framework is validated on a simple plated structure [23] and the results show that the proposed optimization framework is robust and able to predict the expected stochastic fatigue lives. Subsequently, the proposed optimization framework is applied on an offshore K-node structure designed using cast steel to optimize the location and lengths of the welds based on the fatigue damage.

2. Proposed optimization framework

An optimization framework has been developed for parametrized FE models under cyclic loading [23]. In the framework, a deterministic parameterized FE model is set up including the desired design variables (for example, weld length, thickness, material) and solved for unit loads. From the unit loads, the stresses are extracted and fatigue calculations are performed by superposition of the time histories of the cross-sectional loads. The output of the fatigue calculations is used in the optimization scheme to optimize the
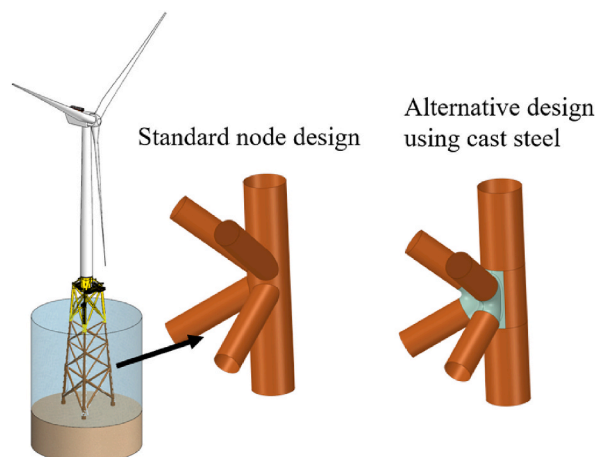

Fig. 1. Standard node design and alternative design using casting.

structure. Oest et al. [4] optimized a jacket structure by considering the fatigue life of the welded joints. In this work, the fatigue stresses were taken as normal-to-weld stresses. Oest and Lund [5] performed topology optimization with finite-life fatigue constraints using the Sines method [24]. Suresh et al. [6] did topology optimization by considering an evolution-based damage model of simple L-beams. Motlag et al. [7] optimized an offshore jacket platform using a genetic algorithm by considering fatigue constraints. Chew et al. [8] presented an analytical gradient-based approach for offshore support structures. These proposed approaches are limited to specific fatigue criteria or stress estimation approaches and considers deterministic analysis. This limit their applicability in real-life design, when the considered guidelines and recommendations often are subjected to updates and changes.

A flowchart of the developed optimization framework is shown in Fig. 2. The proposed optimization framework is an iterative process, and it stops when an optimized solution is reached. The fatigue toolbox in Fig. 2 is used to carry out the necessary fatigue calculations and combining the stress results from the FE model with the external loading. Additionally, the stochastic modelling and analysis are performed in this toolbox. The toolbox makes use of the influence matrix approach [25], which requires external cross-sectional loads to be multiplied with the influence matrices. The resulting damages or fatigue lives are then exported to an optimization handler, which controls the optimization.

To allow for multiple different fatigue criteria and response outputs, the developed framework evaluates the gradients using the finite-difference approach in Eq. (1).

$$\left.\frac{\partial f}{\partial x_i}\right|_{\mathbf{X}_m} \simeq \frac{f(\mathbf{X}_m + \Delta x_i) + f(\mathbf{X}_m)}{\Delta x_i}, \quad i = 1, 2, 3 \ldots, n \tag{1}$$

Where $\frac{\partial f}{\partial x_i}$ is the gradient evaluated at X_m and Δx_i is a small step for one of the considered design variables, x_i. $f(\cdot)$ is the response function being evaluated, such as the fatigue life or fatigue damage. The benefit of the finite-difference approach is that it is very easy to implement and analytical gradients are not required. However, it increases the computation time, because the finite-difference equation must be evaluated $n + 1$ times, where n is the number of considered design variables.

2.1. Fatigue calculations

To perform the fatigue optimization in the framework shown in Fig. 2, a fatigue toolbox has been developed. The purpose of the toolbox is to perform the required fatigue analysis based on the results from the FE model and the external load-time histories. From the FE model and load input, the stress histories are calculated and evaluated using the considered fatigue criterion. In Ref. [23], the authors used the developed framework in combination with 4 different fatigue criteria on a simple plate structure. In that investigation the fatigue life was considered deterministic and did not take into account that longer welds usually result in earlier failure. In this paper, the welds are optimized by also considering the stochastic size effect and for this reason only a single fatigue criterion is considered in the optimization. The governing criterion from the IIW [10] also known as the Gough-Pollard [26] equation is used:

$$\left(\frac{\Delta\sigma_x}{\Delta\sigma_R}\right)^2 + \left(\frac{\Delta\tau_{xy}}{\Delta\tau_R}\right)^2 \leq CV \tag{2}$$

where $\Delta\sigma_x$ and $\Delta\tau_{xy}$ are the normal stress range perpendicular to the weld and shear stress range, respectively. The normal stress ranges and shear stress ranges are found based on rainflow counting in accordance to the ASTM code [27]. The values $\Delta\sigma_R$ and $\Delta\tau_R$ are the
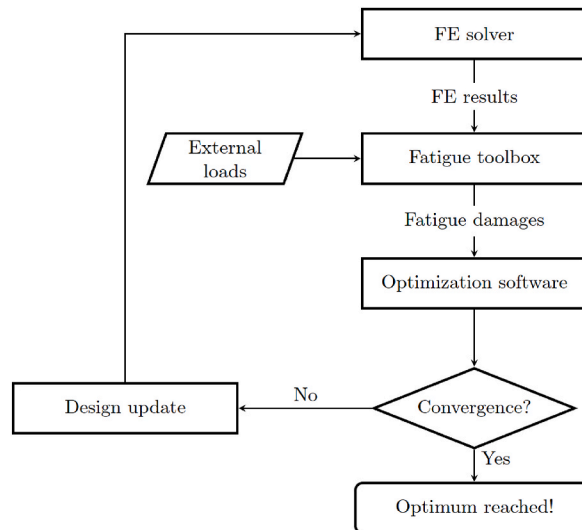

Fig. 2. Flowchart of the developed optimization framework for fatigue optimization.

normal stress fatigue strength and shear stress fatigue strength at a given number of cycles N respectively. CV is called the comparison value, which is equal to 1 for proportional constant amplitude loading and equal to 0.5 for non-proportional loading [10]. The Gough-Pollard equation is proposed for welded structures in accordance with IIW recommendations [10]. This approach can be used, where the welded structures are in the linear-elastic stress range. Additionally, it can be observed from Eq. (2) that only the perpendicular and shear stresses are considered, excluding any parallel (or hoop) stresses. Thus, in cases where high parallel stress ranges are observed, the Gough-Pollard equation is questionable. The DVS [28] has proposed a method, which also includes the parallel stresses in the Gough-Pollard equation. However, to the knowledge of the authors, this approach has not yet been validated. Therefore, the Gough-Pollard equation is used as reference fatigue criterion in this paper, but the DVS approach can easily be implemented in the proposed optimization framework.

In the case of variable amplitude non-proportional loading, the IIW suggest replacing $\Delta\sigma_x$ and $\Delta\tau_{xy}$, with the equivalent constant amplitude stress ranges $\Delta\sigma_{eq}$ and $\Delta\tau_{eq}$, including the specified damage sum, D_{spec}:

$$\Delta\sigma_{eq} = \sqrt[m_1]{\frac{1}{D_{spec}} \frac{\sum(n_i \cdot \Delta\sigma_i{}^{m_1}) + \Delta\sigma_L{}^{(m_1-m_2)} \cdot \sum\left(n_j \cdot \Delta\sigma_j{}^{m_2}\right)}{\sum n_i + \sum n_j}} \qquad (3)$$

Where $\Delta\sigma_i$ and $\Delta\sigma_j$ is the stress ranges above and below the knee-point of the S–N curve, respectively. n_i and n_j are the corresponding number of applied load cycles. Eq. (3) should be calculated for $\Delta\sigma_{eq} > \Delta\sigma_L$, where $\Delta\sigma_L$ is the fatigue strength at the knee point of the S–N curve. If $\Delta\sigma_{eq} < \Delta\sigma_L$, Eq. (4) should be used instead.

$$\Delta\sigma_{eq} = \sqrt[m_2]{\frac{1}{D_{spec}} \frac{\Delta\sigma_L{}^{(m_2-m_1)} \cdot \sum(n_i \cdot \Delta\sigma_i{}^{m_i}) + \sum\left(n_j \cdot \Delta\sigma_j{}^{m_2}\right)+}{\sum n_i + \sum n_j}} \qquad (4)$$

where D_{spec} varies between 0.2 and 1 in accordance with the IIW [10] depending on whether variable amplitude loading is observed. For simplicity, the value of D_{spec} has been kept constant at 1 in the following numerical case studies. This corresponds to the case of constant amplitude loading, however, it will not alter the optimization results as only the reference damages will change. The equivalent shear stress range, $\Delta\tau_{eq}$, can be found similarly.

The IIW criterion and other fatigue criteria in literature depends on the normal-to-weld stresses [10–12] and corresponding shear stresses, thus it is crucial that the normal-to-weld direction can be determined automatically in the optimization framework. To automatically do so, the fatigue toolbox uses a simple algorithm to identify the correct normal-to-weld direction. The algorithm utilizes the fact that on the surface of a structure, the third principal stress is zero unless external loading is applied on the surface. Additionally, it is based on the principle, that a weld is defined by multiple nodes in the FE model. This means that a weld is defined by a line of nodes. Using the closest neighbour of the node, the parallel stress direction can be determined. Firstly, the z-axis (face normal) is determined by calculating the principal stresses and its directions from an arbitrary load step. These can be determined using the eigenvalue problem:

$$\boldsymbol{\sigma}_n \cdot \mathbf{n} = \lambda_P \cdot \mathbf{n} \qquad (5)$$

where $\boldsymbol{\sigma}_n$ is the stress tensor at the considered node, for an arbitrary load case. n is the eigenvector, corresponding to the principal directions and λ_P is the eigenvalues that correspond to the principal stresses. From the eigenvalue problem, the z-axis can be deter-
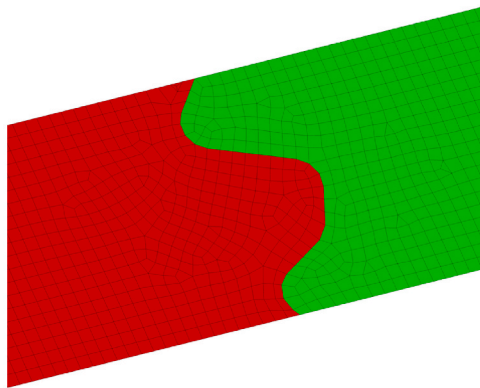
(a) FE model used for automatic weld plane

detection.
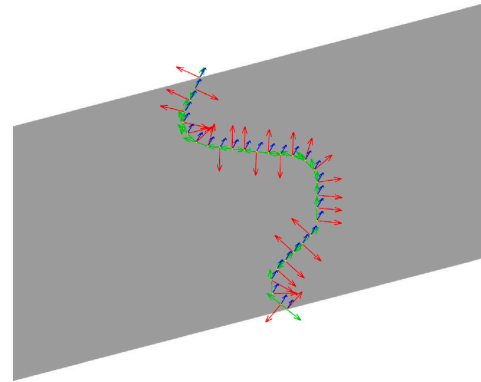
(b) Automatically generated coordinate

systems.

Fig. 3. Example of plate with a random weld line (a) and automatically determined coordinate systems (b).

mined by the axis where the principal stress is zero. In practice, due to the small numerical errors that can be expected from the FE models, the third principal stress will not give exactly the value of zero, thus the smallest absolute number can be used to define the third axis. From the definition of the third axis (z-axis), it is possible to determine the y-axis of the coordinate system as the direction towards the closest neighbouring FE node. This is possible as a weld is defined as a path of FE nodes. Finally, the first axis (x-axis) can be defined based on the other two vectors using general vector calculations:

$$\mathbf{n_x} = \frac{\mathbf{n_y} \times \mathbf{n_z}}{\left| \mathbf{n_y} \times \mathbf{n_z} \right|} \tag{6}$$

Thus, at each node in the weld a coordinate system can be generated, where the x-axis is normal to the weld, the y-axis follows the weld-length direction, and the z-axis is normal to the surface.

Fig. 3 (a) shows a simple plate in which fictitious random weld line is modelled and Fig. 3 (b) shows the corresponding automatically detected coordinate systems. As shown in Fig. 3 (b), the algorithm does not determine a consistent x-axis, as the z-axis and y-axis can vary, however, the x-axis is always normal to the weld line.

After orientating the nodal coordinate systems, the stresses can be extracted for fatigue analysis. In the FE model, only a limited amount of load cases is applied to reduce the calculation time. The influence matrix approach is utilized, which relates certain loads to the stress components at the nodes [25]. The stress tensor at a specific node can then be described as a product of the influence matrix IM and the forces acting on the structure $\mathscr{F}$:

$$\boldsymbol{\sigma}' = \mathbf{IM} \cdot \mathscr{F} \tag{7}$$

For the case of a 2D stress state Eq. (7) can be exemplified by Eq. (8).

$$\boldsymbol{\sigma}' = \begin{bmatrix} \sigma_x \\ \sigma_y \\ \tau_{xy} \end{bmatrix} = \begin{bmatrix} \alpha_{11} & \alpha_{12} & \alpha_{13} \\ \alpha_{21} & \alpha_{22} & \alpha_{23} \\ \alpha_{31} & \alpha_{32} & \alpha_{33} \end{bmatrix} \cdot \begin{bmatrix} F_1 \\ F_2 \\ F_3 \end{bmatrix} \tag{8}$$

where each α_{xy} parameter describes the influence from the load (y) to the stress component (x). For a 3-dimensional stress state, the influence matrix will have the size of 6xM where M is the number of input forces, $\mathscr{F}$. The benefit of using the influence matrix approach is that the evaluation of the stress-time series is based on a limited number of load cases solved in the FE model, as the stress evaluation is performed simply by matrix multiplication. Additionally, it makes it possible to use different finite element software such as ANSYS [29], Abaqus [30] and OptiStruct [31] as the output is comparable. This approach can only be used when the FE models are linear-elastic.

3. Randomness in welded structures

Welded structures are exposed to randomness which results in variation in the fatigue life of the structure. The randomness can be divided into three groups based on the type of origin. The groups consist of: the weld properties, the geometry [13] and the external sources as shown in Fig. 4. The three groups are not completely independent. For example, the randomness in the weld shape (geometry) can be included by the stress estimation approach which can be considered an external source of randomness [13]. Some examples of the uncertainties under each main group are shown in Fig. 4.

All three categories influence the S–N curves, which are used as input in the fatigue calculations. The design S–N curves provided in the governing guidelines and recommendations in the IIW [10] or DNV [11], takes into account many of the uncertainties exemplified in Fig. 4. The randomness in weld properties and weld material is handled in the S–N curves by performing a large amount of fatigue experiments and using the 97.7% fatigue strength which results in a probability of failure of only 2.3%. The weld shape is also
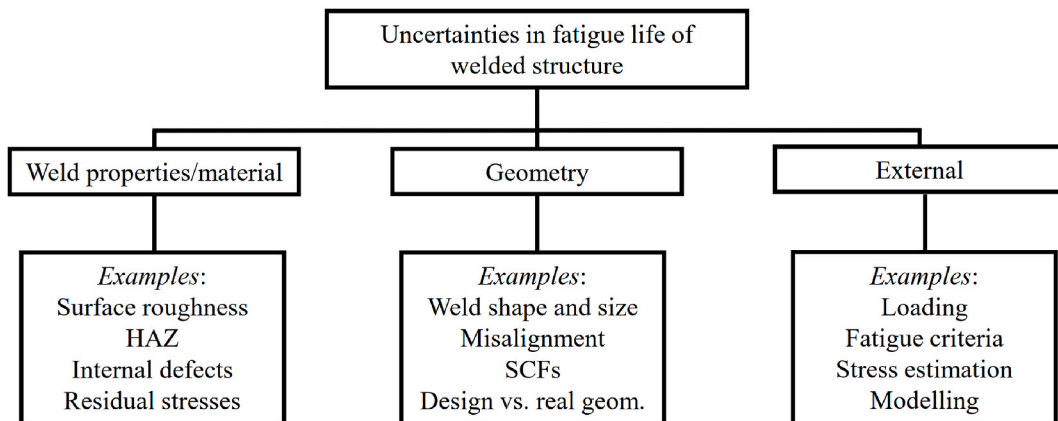

Fig. 4. Different sources of uncertainty in the fatigue life of welded structures.

considered by including an inherent stress concentration factor (SCF) in the S–N curves [11] depending on the stress estimation method. The SCF is an additional stress factor to be multiplied with the estimated stress to take into account effects such as geometrical stress raisers [11]. External uncertainty from the loading and fatigue criteria is considered by safety factors.

A special consideration for welded structures is the size effect (also sometimes denoted thickness effect) [10–12]. This effect considers that the wider, thicker and longer welds in joints are more prone to fatigue damage than narrower and shorter welds. This is often attributed to three effects, namely the geometric size effect, the technological size effect and the statistical size effect [14].

The geometric size effect takes into account that as the thickness of the plate increases, the stresses occurs over a larger thickness near the surface of the plate as compared to smaller plate thicknesses, which leads to lower fatigue lives [14,32]. Additionally, the weld shape (toe angle, radius and undercut) does not scale with the increased thickness of the plate. The technological size effect takes into account the different manufacturing conditions for thinner and thicker welded joints. In these cases, the residual stresses are considered important by some authors [14], while other authors argue that the residual stresses are not an important parameter as given in the review by Lotsberg [32]. Residual stresses are known to influence the fatigue life by altering the state of mean stresses, however, this is often considered a deterministic effect [10,11]. Therefore, it has been neglected in the formulation of the stochastic size effect. The effect of residual stresses (mean stresses) can, be adopted in the optimization framework using the deterministic approaches.

Weld fatigue can be considered a weakest link process, where the worst combination of stresses, defects and material properties result in crack initiation [14,32]. The uncertainty in these parameters can be described by the statistical size effect. An example is provided in Fig. 5 (a), where a large plate with a single weld defect (indicated with a red mark) is shown. If the single plate is tested in fatigue, the plate will fail at the weld defect, at an earlier cycle number than expected. However, if the specimen is divided into six equally wide specimens as shown in Fig. 5 (b), only one of the specimens will fail earlier than expected and thus reducing the probability of failure considerably. Therefore, shorter welds show better fatigue performance than longer welds.

The size effect is considered deterministic by the DNV by increasing the effective stress range in the fatigue calculations in Eq. (9) [11].

$$\Delta \sigma_{eff} = \left(\frac{t}{t_{ref}}\right)^k \cdot \Delta \sigma, \quad t > t_{ref} \tag{9}$$

where $\Delta \sigma$ is the occurring stress range, t is the plate thickness, t_{ref}, is the reference thickness which depends on connection type and k is the thickness exponent depending on the detail category. Eq. (9) is a deterministic approach for handling the combined size effect, where the statistical size effect is not considered explicitly. In the DNV guidance, some efforts of including the statistical size effect have been made based on the weld length. However, the recommendations are only to be used in cases where test data is not comparable to the larger-scale real structures [11]. Thus, in practical fatigue life calculations of offshore welded joints, the length effect is neglected.

In the case of welded joints, the statistical size effect is governed by the weld length and not the weld volume as discussed in Refs. [14,15,33].

3.1. Modelling of statistical size effect

Random fields (randomness as a function of for example length, time or multiple dimensions) can be discretized into random variables using the Karhunen-Loéve (KL) expansion [34]. The expansion is often used in combination with the stochastic finite element method (SFEM) [17,18,35]. The KL expansion makes it possible to account for randomness as a function as in the case of the statistical
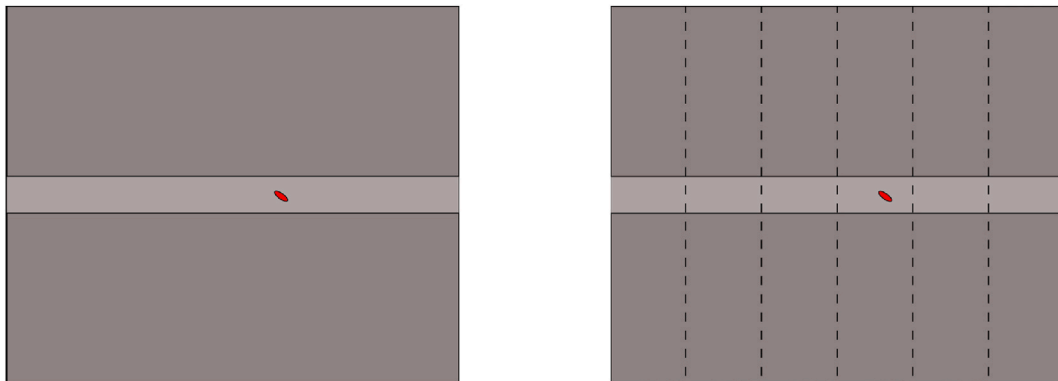
(a) Single large specimen.   (b) Six smaller specimens.

Fig. 5. Statistical size effect on a large plate with defect (a) and smaller plates (b), adapted from Ref. [14].

size effect. In this paper, the statistical size effect is modelled using the KL expansion and it is used in the optimization framework. The statistical size effect is modelled as a one-dimensional field as a function of the length of the considered welds. This corresponds to the literature indicating that the statistical size effect is governed by the length and not by the volume [14,15,33]. To the best of knowledge of the authors, no efforts have been made in modelling the statistical size effect using the KL expansion.

Different approaches for modelling the statistical size effect can be chosen. In the DNV standard [11], the reduction in fatigue strength is considered by Eq. (9) by adding an additional factor to the input stress. A similar approach is used in this paper, where the statistical size effect is modelled as an additional stress concentration factor which should be added to the estimated stress ranges, as expressed in Eq. (10).

$$\Delta\sigma_{eff} = \text{SCF}_S(x,\theta) \cdot \Delta\sigma \tag{10}$$

where $\Delta\sigma$ is the stress range, $SCF_S(x,\theta)$ is the stochastic stress concentration factor for the size effect and subscript S denotes stochastic. SCF_S is to be added to all stress components, including shear stresses. x is the domain of the field, which corresponds to the length of the weld. θ is an outcome from the random sample space ω, thus $\theta \in \omega$. Each realization θ_i corresponds to a single stochastic SCF function $SCF_S(x,\theta_i)$. The formulation given in Eq. (10) is a simplification, as the randomness in the fatigue life of the welds can be caused by both additional stress concentrations but also material randomness and weld defects as shown in Fig. 4. However, it is assumed that the effect of the randomness in the material and weld defects, can be simulated using additional stress concentration factors.

The random field $SCF_S(x,\theta)$ is discretized using the Karhunen-Loéve expansion [34,36]. The KL expansions is a generalized Fourier type series based on the decomposition of the covariance function. The KL expansion can be expressed as:

$$F(\mathbf{r},\theta) = F_0(\mathbf{r}) + \sum_{j=1}^{\infty} \sqrt{\lambda_j}\xi(\theta)\varphi_j(\mathbf{r}) \tag{11}$$

Where λ_j and $\varphi_j(r)$ are the eigenvalues and eigenfunctions to the integral equation in Eq. (12). $F_0(r)$ is the deterministic part of the field and $\xi_j(\theta)$ are uncorrelated random variables. The integral equation expressed in Eq. (12) is a Fredholm integral of the second kind.

$$\int_{\mathscr{D}} C_f(\mathbf{r}_1,\mathbf{r}_2)\varphi_j(\mathbf{r}_1)d\mathbf{r}_1 = \lambda_j\varphi_j(\mathbf{r}_2), \quad \forall j = 1,2,\dots \tag{12}$$

Where C_f is the autocovariance function. The Fredholm integral can be difficult to solve analytically, however, several numerical methods have been proposed in literature [37,38]. In this paper, only the length of the weld is considered in the stochastic field, thus resulting in Eq. (11) being a one-dimensional random field. Analytical solutions to one-dimensional random fields have been presented in literature [39,40]. In the case of an exponential autocovariance function given in Eq. (13) as:

$$C_f(x_1,x_2) = \exp\left(\frac{-|x_1 - x_2|}{b}\right) \tag{13}$$

where b is the correlation length. The correlation length describes the rate at which the correlation function decays between two points in the random field. The covariance field become more correlated with increase in correlation length. By increasing the correlation length b, the random field behaves as a single random variable.

The random field can be expanded by considering a zero mean in the domain $-a \le x \le a$:

$$F(x,\theta) = \sum_{j=1}^{\infty} \sqrt{\lambda_j}\xi(\theta)\varphi_j(x) \tag{14}$$

where the eigenvalues λ_j and eigenfunctions φ_j are calculated using Eq. (15) for odd j and Eq. (16) for even j [16,35,40]. a corresponds to the considered domain and in the case of a 1D domain (such as the length of a weld), a corresponds to the full length of the weld.

$$\lambda_j = \frac{2c}{\omega_j^2 + c^2}, \quad \varphi_j(x) = \frac{\cos(\omega_j x)}{\sqrt{a + \frac{\sin(2\omega_j a)}{2\omega_j}}} \quad \text{where} \quad \tan(\omega_j a) = \frac{c}{\omega_j} \tag{15}$$

$$\lambda_j = \frac{2c}{\omega_j^2 + c^2}, \quad \varphi_j(x) = \frac{\sin(\omega_j x)}{\sqrt{a - \frac{\sin(2\omega_j a)}{2\omega_j}}} \quad \text{where} \quad \tan(\omega_j a) = \frac{\omega_j}{-c} \tag{16}$$

where $c = 1/b$. For practical use, the KL expansion needs to be truncated to a finite number of terms. The required number of terms depends on the desired level of information to be kept [40,41]. If only 10% of the information is desired to be retained, the required number of KL terms can be determined as $\sqrt{\lambda_N}/\sqrt{\lambda_1} = 0.1$ [40,41]. In this case, the last KL term will include 10% information as compared to the first and most influencing term.

Using the KL expansion approach, the stochastic SCF can be expressed as:

$$\mathrm{SCF}_S(x,\theta) = \mathrm{SCF}_0(1 + \varepsilon_1 F_1(x,\theta)) \tag{17}$$

where ε_1 is a deterministic constant, given as $0 < \varepsilon_1 \ll 1$. ε_1 is a strength parameter that quantifies the randomness in the random field, if $F_1(x,\theta)$ is considered to have zero mean with a unit standard deviation [40]. SCF_0 is the mean value of the stress concentration factor. The strength parameter ε_1 is comparable to the coefficient of variation (CoV) of the stochastic field. Thus, the stochastic fluctuations are determined by F_1 and the strength (magnitude) of the fluctuations is determined by ε_1.

The benefit of using the KL expansion approach to discretize the stochastic field as compared to a more general direct Monte Carlo (MC) simulation approach is that KL expansion approach requires a reduced number of random variables. For example, if the considered weld consists of 100 nodes at which the fatigue damage should be evaluated, 100 random variables will be required for generating the random SCFs, which is used to model the statistical size effect with the MC approach. Using 10,000 MC simulations will result into a total of $10,0 \times 10,000 = 1,000,000$ required random samples. If the KL expansion is used instead, the amount of required random variables correspond to the number of required KL terms. Each KL term needs a random variable $\xi_j(\theta)$ as given in Eq. (14), thus making it independent of the number of nodes (or evaluation points) in the weld. Thus, if 100 nodes are considered in the weld and 14 kL terms is required, only $14 \times 10,000 = 140,000$ MC simulations are required.

The statistical size effect modelled as an SCF is especially useful in the case of the IIW fatigue criterion given in Eq. (2). Here, the additional SCF can be included in both the normal stress and the shear stress terms as:

$$\left(\frac{\Delta\sigma_x \cdot SCF_S(x,\theta)}{\Delta\sigma_R}\right)^2 + \left(\frac{\Delta\tau_{xy} \cdot SCF_S(x,\theta)}{\Delta\tau_R}\right)^2 \leq CV \tag{18}$$

This is equivalent to stochastically varying the fatigue strengths $\Delta\sigma_R$ and $\Delta\tau_R$. This corresponds to the case, where a defect in the weld influences the resulting fatigue strength equally for both shear and normal stresses. Some efforts have been made in modelling the fatigue life as a stochastic field using the KL expansion. Liu and Mahadevan [42,43] used the KL expansion to develop the so-called stochastic S–N curve approach, where the variability in the S–N curves for damage accumulation is taken into account. However, in this approach, the S–N curves are considered random over the lifetime cycles. In the proposed approach, the S–N curves (fatigue strengths) are considered constant for each node but varies over the length of the weld, thus varies over the nodes. This makes it possible to model the randomness in the weld as a function of the weld instead of modelling it as a function of the fatigue strength. The benefit of this approach is that the physical correlation between locations in the weld can be taken into account, instead of treating each node in the weld as an independent node.

4. Case study of a simple plate structure

In this section, a numerical case study of a simple plate structure is optimized for the weld orientation. The plate structure is used to validate the optimization framework, as fatigue results can easily be calculated by hand. In sub-section 4.1, a deterministic optimization of the weld orientation is performed and in sub-section 4.2, the optimization is performed considering the stochastic size effect.

The simple plate [23] is optimized for weld orientation considering the fatigue damage. The plate consists of two parts, which are welded together as shown in Fig. 6. The weld is assumed to be a butt weld in accordance with the FAT-90 S–N curve for normal stresses and the FAT-80 S–N curve for shear stresses [10].

The simple plate is assumed to be deterministically uniaxially loaded as shown in Fig. 7. The deterministic loading is given as:

$$F(t) = 65\,\mathrm{kN} \cdot \sin(2\pi \cdot t), \quad 0 \leq t \leq 1.0 \times 10^5 \tag{19}$$

Thus, a total of 100,000 load cycles have been applied with a load amplitude of 65 kN resulting in a load range of 130 kN.

The FE model is shown in Fig. 7 and it has been created using the commercial OptiStruct software [31]. A total of 1600 shell elements have been used with 1710 corresponding nodes. A linear elastic material model is used with Young's modulus of $E = 210\,GPa$ and Poissons number $\nu = 0.3$.

In the optimization, the design variable is the weld orientation, which allows for the weld to rotate up to 45° around the centre of the plate. This is achieved by controlling the endpoints of the weld using two shape parameters, which alter the weld orientation angle β, as shown in Fig. 7. The shape parameters, S_1 and S_2, can move a total of 50 mm to achieve 45° orientation. The parameters are coupled, thus S_1 moves consistently with S_2. The objective of the optimization is to minimize the estimated fatigue damages in the weld. Thus, all nodes in the weld line are analysed for fatigue damage and the maximum is minimized. In total, 21 nodes are examined
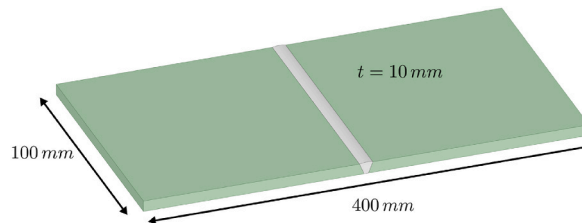

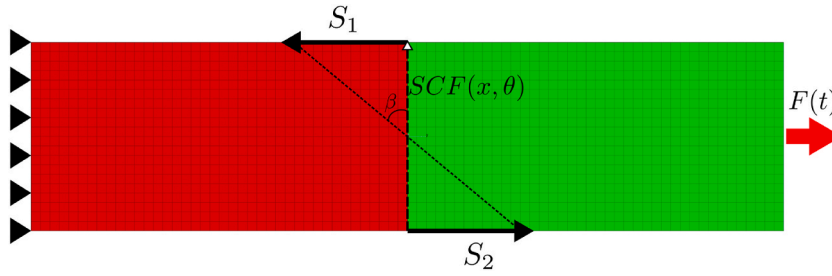**Fig. 6.** Welded plate structure considered for fatigue optimization.

Fig. 7. Finite element model of the simple plate including designation of shape parameters and stochastic SCFs.

in the fatigue analysis. In the simple plate, as no geometrical features lead to varying stress states in the weld, the 21 examined nodes will lead to the same fatigue damage with small variations caused by the numerical model.

4.1. Deterministic optimization

In this investigation, the optimization is performed without considering any randomness, to validate the optimization framework. The fatigue performance is evaluated using the IIW criterion by calculating an equivalent damage. By rearranging the Gough-Pollard equation in Eq. (2), an equivalent damage can be obtained as:

$$\frac{1}{CV}\left(\left(\frac{\Delta\sigma_x}{\Delta\sigma_R}\right)^2 + \left(\frac{\Delta\tau_{xy}}{\Delta\tau_R}\right)^2\right) = D_{eq} \tag{20}$$

It should be noted that Eq. (20) is an equivalent damage estimator which cannot directly be compared to damages estimated using the Palmgren-Miner rule [44]. In Eq. (20), $\Delta\sigma_x$ and $\Delta\tau_{xy}$, corresponds to the normal stress and shear stress range respectively in the direction perpendicular to the weld, thus utilizing the automatic determination of the orientation described in sub-section 2.1. The reference stress ranges $\Delta\sigma_R$ and $\Delta\tau_R$ are determined as the fatigue strength at the number of applied cycles for the normal stress S–N and shear stress S–N curves, respectively.

No additional SCF is included in the stress estimation as the statistical size effect is neglected.

In Table 1, the original and optimized results from the deterministic optimization are presented including the estimated stress ranges. It can be observed from Table 1, that the optimization leads to a reduced fatigue damage, when the weld is oriented at 45° from the original location. Furthermore, it can also be observed that the equivalent damage from the FE analysis and the analytical calculations are identical. As the S–N curves are not varied in the optimization, the optimized weld orientation will be at 45° as the normal-to-weld stress are reduced considerably.

The optimization has been performed using the Global Response Search Method (GRSM) [45] using 15 fixed iterations. The GRSM optimization procedure is useful in fatigue problems as the algorithm uses global sampling so the global minima/maxima are more likely to be found. The iterative results are shown in Fig. 8 (a), where the fatigue damage is plotted vs the rotation of the weld. As seen from Fig. 8 (a), the optimized weld orientation is already found in iteration number 4, however, as the GRSM approach searches for a fixed number of iterations, the optimization continued. In the optimization, the weld is allowed to rotate ±45°, thus symmetrical results are observed. The optimized weld orientation in the FE model is shown in Fig. 8 (b). As observed in Fig. 8 (a), the damage increases between iteration 1 and iteration 11 (and 9). Thus, if a local optimization approach is used, without global checks, the optimal orientation of the weld will be found at 0° instead of 45°. In that case, no optimum can be found.

4.2. Optimization considering the stochastic size effect

In this investigation, the shape optimization presented above is expanded to include stochastic SCFs modelled using the KL expansion. The stochastic SCFs are used to simulate the statistical size effect as explained in Section 3. The weld quality is often highly dependent on the welder's skills (if manually welded), the welding type, the material etc. thus a great variety of statistical input properties can be expected in real life. The stochastic properties used in the optimization are listed in Table 2. To the knowledge of the authors, no investigations have previously been carried out by considering the weld line as stochastic. Thus, the values considered in this investigation are used to demonstrate the effect of correlation length and coefficient of variation on the resulting fatigue damages. Note that the STD and the CoV are proportional as *CoV = STD/Mean*. The stochastic SCFs provided in Table 2 are applied to both the

Table 1
Optimization results from deterministic optimization of simple plate.

Orientation	$\Delta\sigma_x$	$\Delta\tau_{xy}$	Equivalent damage D_{eq} from FEA.	Analytical equivalent damage D_{eq}	Deviation
0°	130 MPa	0 MPa	0.283	0.283	0.00%
45°	65 MPa	65 MPa	0.270	0.270	0.00%
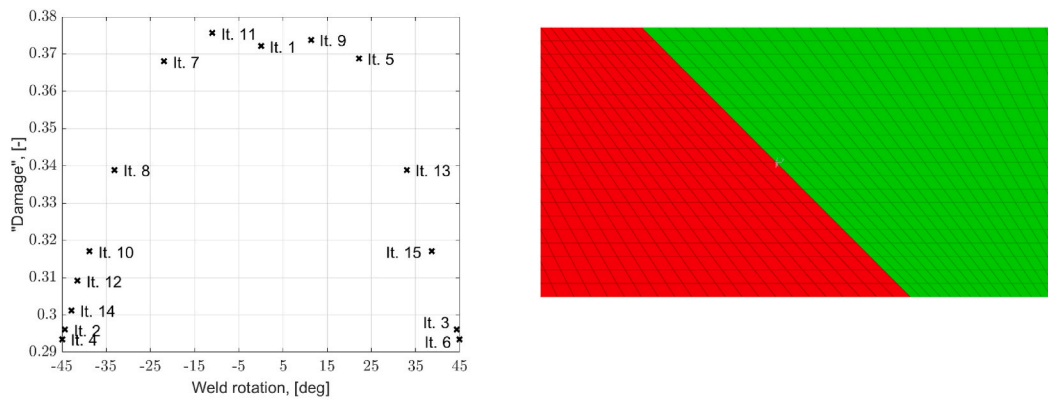
(a) Predicted damage from each iteration of the optimization.

(b) Optimized weld orientation of FE model.

Fig. 8. Optimization results of simple plate considering weld orientation (a) and optimized weld orientation (b).

Table 2
Stochastic input parameters for the optimization of the simple plate.

Property	Distribution	Mean	STD	CoV	Correlation length, b
Stress concentration factor, SCF	Gaussian	1.00	0.02, 0.05, 0.10	CoV = (2%, 5%, 10%)	b = (L/5, L/2, L), L = 0.1 m

normal stress ranges and the shear stress ranges in accordance to Eq. (18). This means that the normal stress and shear stress fatigue strengths are reduced or increased stochastically in an equal manner. An increase in CoV/STD results in more variation in the SCFs, similar to the case of single random variables. Increasing the correlation length b results in a more correlated field.

During the optimization the weld orientation is rotated, which leads to longer welds. A longer weld results in different fatigue lives than for a shorter weld when the statistical size effect is considered. The interrelation between weld length and statistical properties are controlled by the correlation length.

The KL expansion of the stress concentration factor given in Eq. (17) is used to discretize the stochastic size effect. Thus, the stochastic field is discretized using Eq. (14) and it is multiplied with the strength parameter (CoV given in Table 2). The KL expansion is truncated to obtain a 10% of retained information, which depends on the correlation length and the coefficient of variation of the input statistics. Additionally, it also depends on the length of the weld. When the weld is rotated 45°, the length of the weld is approximately 40 mm longer than in its original state. Thus, the increase in length results in more KL terms required to obtain 10% of the retained information. This is handled automatically in the proposed optimization framework.
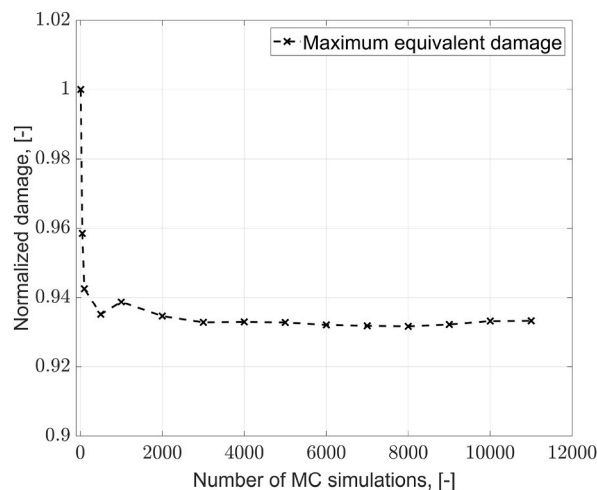

Fig. 9. Convergence study of normalized maximum damage over all 21 nodes, considering stochastic SCFs with b = 1/5L and CoV = 10%.

In the optimization, the Monte Carlo simulation approach is used for generating the random samples $\xi_j(\theta)$ to generate the stochastic SCFs. In total 10,000 MC simulations is used for each stochastic analysis. As a fatigue failure will occur at the location of the highest damage, for each MC simulation the maximum damage over the 21 investigated nodes is predicted and it is used in the statistical evaluation. To validate the required number of MC simulations, a convergence study is performed. The mean of the maximum equivalent damage from all MC simulations and all nodes is plotted in Fig. 9 for different amounts of MC simulations. The MC convergence study is performed with b = L/5 and CoV = 10%, which requires the highest amount of MC simulations. As seen from Fig. 9, the equivalent damage stabilizes at around 3000 MC simulations. Using 10,000 samples ensures that even when rotating the weld, the results converge.

In Table 3, the optimized results are shown for various combinations of statistical input parameters. The results consist of the mean of the maximum calculated damage and the corresponding standard deviation. As observed from Table 3, the mean equivalent damage reduces with a lower coefficient of variation. This is consistent with the fact that fatigue is a weakest link process. A higher CoV results in a higher risk of having a high SCF and thus a lower fatigue life. It can also be observed from Table 3 that with decreasing correlation length, higher equivalent damages are found. This corresponds to the case, where there is a lesser control over the welding process and thus a higher risk of a defect in the weld. In Table 3, the difference in mean damages is also shown. The difference is predicted individually for the case of CoV = 2%, CoV = 5% and CoV = 10%. The results show that an increase in the correlation length b results in reduced equivalent damages. This effect is more noticeable with increasing CoV, as the strength of the stochastic fluctuations are increased and thereby resulting in increased risk of high damage. In the case of CoV = 10%, it can be observed that by increasing the correlation length b = L, it will reduce the equivalent damage by approximately 11%. The same trends are observed for both the unoptimized and optimized solutions. In the case of optimization number 4, a very high correlation length has been used. This simulates the case where the weld properties are constant over the length of the weld, thus behaving as a single random variable. In that case, it is expected that the mean equivalent damage should be corresponding to the deterministic damages presented in Table 1. As seen from the tables, this is true as only minor differences are observed in the third decimal.

In Fig. 10, the results for the optimization using a CoV of 5% are presented for the different considered correlation lengths. As observed from Fig. 10, the overall shapes of the optimization results are similar, with the main difference being that smaller correlation length results in higher mean damages (as also observed in Table 3). This clearly shows that using consistent welding results in lower fatigue damages and higher fatigue lives. It should be noted that due to the symmetry conditions, the optimization is performed for weld orientation angles between 0 and 45°. As the weld length increases during the optimization, the effect of decreased correlation length is shown in Fig. 11 by normalizing the results to start at the same point as the results using b = L. As observed from Fig. 11, the gradients of the results with lower correlation lengths increase with increased weld length. However, it is observed that the effect decreases from around weld orientations of 30° up to 45°. This is caused by the fact that at this rotation, the shear stresses dominates in the FE model, thus considerably changing the contribution from normal stresses and shear stresses in Eq. (18). It can be concluded that the use of stochastic formulation of the SCFs to take into account the statistical size effect, allows for modelling the effect of longer welds and lower consistency in the welding.

5. Optimization of cast steel K-Joint in offshore jacket structure

The fatigue optimization framework has been applied on a jacket joint, which is expected to be manufactured in cast steel. The joint is modelled together with a jacket structure originally designed by Ramboll Offshore wind as shown in Fig. 1. Using cast steel allows for a more compact design and better load transfer in the structure. The cast node is to be welded into the rest of the structure, thus the fatigue life at the welds is still one of the important governing parameters. Especially, the welds between the cast steel and the chord (main leg) are of interest as they will be exposed to a large number of fluctuating stresses. The cast joint design is shown in Fig. 12. Only the local joint is considered in the optimization and thus any effect of local changes to the global behaviour is neglected. The global FE model is developed using higher order Timoshenko beam elements with 12° of freedom in the in-house Ramboll software and it is used to estimate the sectional forces at the cut-points of the structure. The cut-points act as connectors to the local FE model and are used in the influence matrix approach.

Table 3
Optimization results using varying statistical input parameters.

| Opt.	CoV	b	Original weld orientation			Optimized weld orientation		
			Mean equivalent damage	STD equivalent damage	Difference in mean damage	Mean equivalent damage	STD equivalent damage	Difference in mean damage
1	2%	L/5	0.299	0.008	Ref.	0.287	0.007	Ref.
2	2%	L/3	0.296	0.009	−1.00%	0.284	0.008	−1.02%
3	2%	L	0.291	0.010	−1.67%	0.279	0.009	−2.79%
4	2%	25L	0.284	0.011	−5.01%	0.271	0.011	−5.57%
5	5%	L/5	0.324	0.021	Ref.	0.312	0.019	Ref.
6	5%	L/3	0.317	0.023	−2.16%	0.307	0.021	−1.60%
7	5%	L	0.304	0.026	−6.17%	0.293	0.024	−6.01%
8	10%	L/5	0.367	0.045	Ref.	0.358	0.041	Ref.
9	10%	L/3	0.353	0.049	−3.81%	0.346	0.044	−3.35%
10	10%	L	0.326	0.054	−11.17%	0.318	0.050	−11.17%
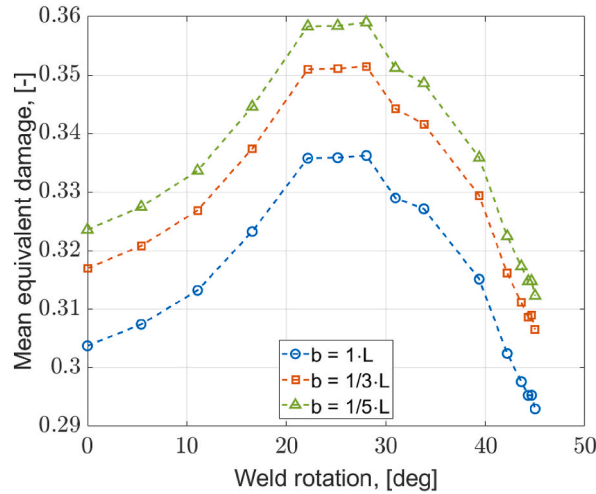
Fig. 10. Results from optimization including stochastic size effect for different correlation lengths and COV = 5%.

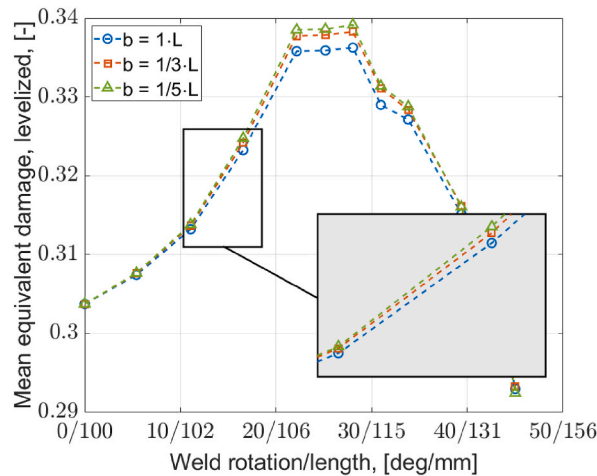**Fig. 11.** Results from optimization including stochastic size effect for different correlation lengths and COV = 5% - Normalized to b = 1 L.

The unoptimized geometry of the structure is shown in Fig. 13. The mass of the cast part is normalized to 1 in the following optimizations due to non-disclosure. The unoptimized design is a shell model, which in real-life structures include bevelling of the plates to obtain better thickness transitions. For simplicity, the bevelling of the thickness is neglected during the optimization, however, the thickness transitions can be made during the casting of the node.

The FE model of the cast node is developed using shell elements as shown in Fig. 14. The number of elements and nodes are listed in Table 4. The use of lower order shell elements instead of solid elements allows for more efficient meshing and thus results in lower computational cost. A material model similar to the regular steel has been applied.

In the optimization, the location and length of the welds in the chord are of interest. The shape of the cast joint is considered fixed. The welds of interest are shown in Fig. 14 (b), marked with red lines. Thus, the welds between the chord and cast part is of interest. The outer edges of the cast part can vary in size and thereby vary the length and location of the welds (parameter P_1 and P_2). The welds at the braces are kept constant during the optimization. The thickness of the chord section is fixed in the optimization for simplicity. However, the thickness of the cast joint can be varied (parameter t). The design variables and the corresponding design lower and upper bound values are listed in Table 5. Discrepancies are expected in the stress results as the stresses are calculated on the weld line. Nodal stresses are calculated by interpolating the stress in the finite elements. The finite element mesh refinement has been carried out to minimize these discrepancies and the maximum calculated error between nodal stresses and elemental stresses is 6%.

Symmetry conditions have been applied so that the top width and bottom width and the left and right height of the welds are kept equal. Thus, the part welded into the chord is kept rectangular.

The structure is analysed for fatigue at the welds highlighted in Fig. 14 (b), which are considered fatigue critical. The welds are evaluated using the IIW approach given in Eq. (20) and the relevant S–N curves for the fatigue analysis are listed in Table 6. The S–N
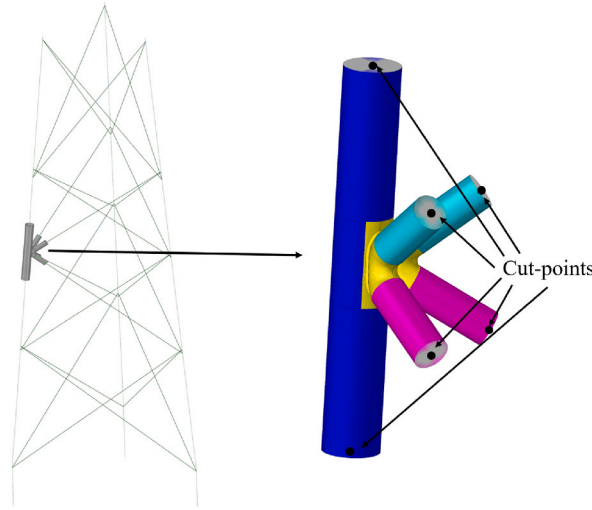
Fig. 12. Finite element model of jacket and corresponding local cast joint model.
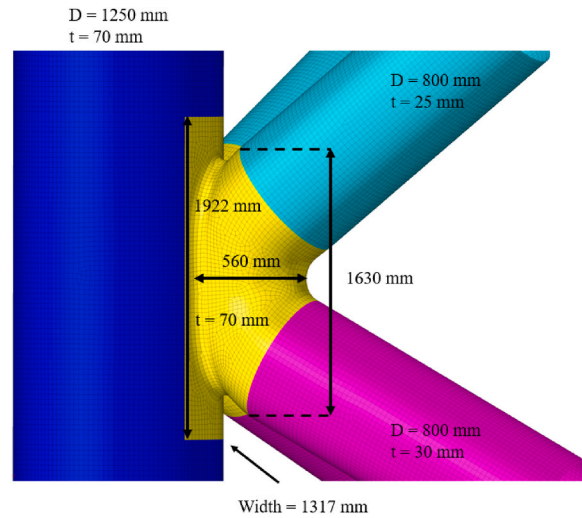

Fig. 13. Preliminary design of the cast joint.

curves are based on the recommendations from the IIW [10] and the DNV [11]. These S–N curves are for normal grade steel and could possibly be different for cast steel, however, this is not considered in this paper. Only the outside of the welds is examined in the optimization. For the vertical and horizontal welds, double-sided full penetration butt welds can be made and thus the FAT-90 normal-to-weld stress S–N curve and the FAT-100 shear S–N curve are used in accordance with the IIW [10]. In Table 6, the corresponding design variable from Fig. 14 (b) are given and the number of evaluated nodes in the FE model for the fatigue analysis is summarized. In total, 260 FE nodes are evaluated during the fatigue analysis.

As the thickness between the welded parts varies, an additional stress concentration factor is considered. The stress concentration factor takes into account any misalignment occurring between the plates and the effect of change in thickness. This factor is assumed deterministic in the optimization. The DNV proposes the following stress concentration factor for welds between plates [11]:

$$SCF = 1 + \frac{6(\delta_m + \delta_t - \delta_0)}{t\left[1 + \frac{T^{1.5}}{t^{1.5}}\right]} \tag{21}$$

where δ_m, δ_t and δ_0 are the misalignment from fabrication, the eccentricity due to thickness change and the misalignment inherent in the S–N data, respectively. T and t are the thickness of the thickest and thinnest parts, respectively. The parameters are shown in Fig. 15. The eccentricity due to thickness change can be calculated as $\delta_t = 1/2\,(T-t)$ and the misalignment inherent in the S–N data can be found as $\delta_0 = 0.05t$ in accordance to the DNV [11]. Eq. (21) has been included in the optimization scheme. For simplicity, the
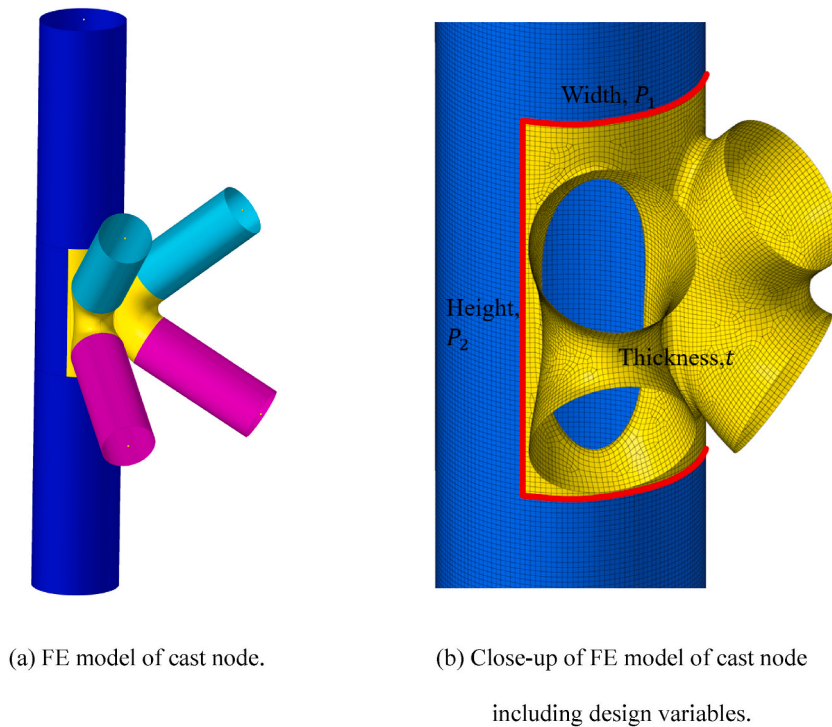
(a) FE model of cast node.

(b) Close-up of FE model of cast node including design variables.

Fig. 14. Finite element model of offshore K-node structure (a) and design variables to control the welds (b).

Table 4
Number of finite elements and nodes used for the cast node design.

Number of Elements	Number of Nodes
87,545	87,992

Table 5
Design variables and lower and upper bound values used for optimization of the cast jacket joint.

Design variables	Description	Lower and upper bound values
P_1	Width of the cast part welded to the chord.	1320 mm (original)-1534 mm
P_2	Height (length) of the cast part welded to the chord.	1922 mm (original)-2721 mm
t	Thickness of the cast part.	55–77 mm (70 mm originally)

Table 6
S–N curves used in optimization of cast jacket joint and corresponding number of evaluated nodes.

Location	Corresponding design variable	Number of evaluated nodes	Normal-to-weld stress S–N curve	Shear stress S–N curve
Horizontal weld	P_1	106	FAT-90	FAT-100
Vertical weld	P_2	154	FAT-90	FAT-100

eccentricity δ_m is assumed to be 4 mm in the following calculations. This allows for calculating reasonable values of SCFs from Eq. (21), however, for other real life welded structures the eccentricity has to be determined from the manufacturing process.

As the cast node is a large scale structure, the effect of residual stresses (or mean stresses in the stress-time series) are neglected in accordance with [10,11].

A jacket structure is exposed to cyclic loading during its full lifetime. This includes cyclic loading during the construction, transportation, installation and in-place phase. The major contribution to the fatigue life is governed by the in-place phase. In this phase, the wind and hydrodynamic loads induce cyclic loading. For more information about fatigue load cases for offshore jacket
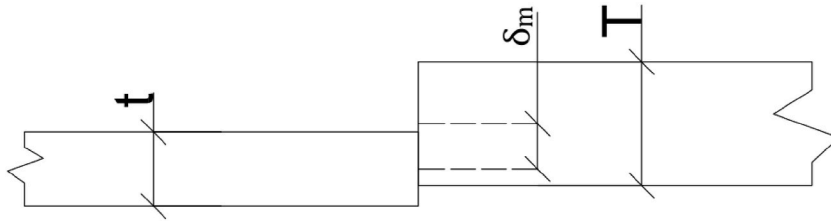
Fig. 15. Parameters used for SCF calculation.

structures, please refer to Refs. [46,47]. For a jacket structure, it is required to evaluate approximately 8000 cases, where each case has a time series of loads. In the Ramboll in-house software for jacket calculations, a load case is 30,000 time-steps long. Thus, in total up to 240 million time-steps have to be evaluated. For an optimization, this is too computationally expensive and thus a representative reduced load case setup has been used in this optimization. The reduced load case setup includes the damage contributions from different loading directions, but with reduced number of load cases. The reduced load cases cannot be used to determine the resulting damage from the full load-time series, however, it gives a good indication of the effect of changes in the weld location on the relative fatigue damage. In total 24 load cases have been considered, corresponding to 740,000 individual time-steps. The 24 load cases are selected based on the rated wind speed for the turbine (14 m/s), 2 yaw angles (−6 and +6°) and 12 wind/wave directions (every 30°). In Fig. 16, an example of the normal and shear stress history in one of the nodes in the welded joint is shown.

5.1. Deterministic optimization

Optimization has been performed by applying the proposed optimization framework. The goal of the optimization is to reduce the mass of the cast part. Thus, the optimization problem can be written as:

$$
\begin{aligned}
\min_{\boldsymbol{x}} \quad & f(\boldsymbol{x}) && \textit{(mass of cast part)} \\
\text{subject to} \quad & D_{Vertical} < D_{Vertical,ref} && \textit{(fatigue damage at vertical welds)} \\
& D_{Horizontal} < D_{Horizontal,ref} && \textit{(fatigue damage at horizontal welds)} \\
& 55\ mm \leq t \leq 77\ mm && \textit{(thickness constraints)} \\
& 1320\ mm \leq P_1 \leq 1534\ mm && \textit{(Width of cast part)} \\
& 1922\ mm \leq P_2 \leq 2721\ mm && \textit{(Height of cast part)}
\end{aligned}
$$

As the load set consists of a reduced setup, the damage constraints cannot be set equal to 1 (fatigue failure in accordance to Eq. (20)). Instead, reference damages are used, which are corresponding to the damage found for the original model for the vertical welds $D_{Vertical,ref}$ and the horizontal welds $D_{Horizontal,ref}$. This means that an optimized design compared to the original unoptimized design is sought. The reference damages are summarized in Table 7. Note, that the maximum damage is used as response and that the output is combined for both horizontal and vertical welds. All nodes in the welds are examined in the fatigue optimization, however, only the
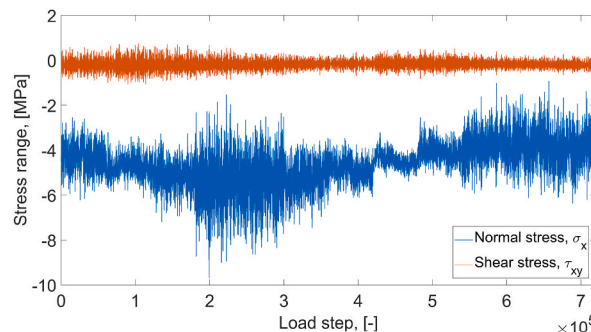

Fig. 16. Example of normal stress and shear stress history for the node in the jacket structure.

Table 7
Reference equivalent damage for original unoptimized design.

Reference damage	Equivalent damage
$D_{Vertical,ref}$	$3.25x10^{-4}$
$D_{Horizontal,ref}$	$1.55x10^{-4}$

maximum damage from all nodes in the welds are used in the response. This means that only one reference damage is found for each set of welds. As seen from Table 7, the reference damages are very small, however they represent the damage from only 0.3% of the full load case series.

The sensitivities of each parameter to the responses (mass and damages) are given in Fig. 17. The sensitivities are calculated based on the finite-difference approach, which uses the lower and upper bound values of each optimization parameter in accordance to Eq. (22), where f is the considered output parameter and P is the input parameter given in Table 5. f_1 corresponds to the lower bound value and f_2 corresponds to the upper bound value of the output parameter. This means that the sensitivity is calculated by considering the lower and upper bound values of the optimization parameter and not the input parameter explicitly. In this investigation, the sensitivities are calculated by percentage change in output function, similar to sensitivity calculation by ANSYS [29]:

$$\frac{\partial f}{\partial P} = \frac{f_2 - f_1}{f_1} \tag{22}$$

The sensitivities are normalized based on the maximum sensitivity in order to make the sensitivities comparable. As observed in Fig. 17, the most influencing parameter on the mass is the thickness t. In case of the vertical weld, it is observed that the damage reduces with increase in width P_1 and thickness t. However, damage increases with increase in height P_2. This is due to the fact that high stresses are observed close to these welds. In case of the horizontal welds, increase in the thickness and height decrease the damage. However, a small increase in damage caused by the width is seen. The sensitivity study also shows that moving the welds further away from the original position (by increasing the lengths), decreases the damage and it allows for thinner designs.

The optimized node is shown in Fig. 18 and the optimized parameters (optimized distances and thickness) are given in Table 8. It can be observed from the results that the mass of the full joint is reduced by approximately 22% and the thickness of the cast part is reduced by approximately 21%. This means a considerable decrease in the material can be obtained by moving the welds further from their original positions. In the optimization, the damages at the weld are at the same levels as the original design.

The optimization performed was carried out on a standard high-performance laptop (i7 2.6 GHz, 48 GB Ram) in approximately 4 h and it took 50 design iterations. This includes analysing the FE model, exporting the stress data, and carrying out the rainflow counting and fatigue life calculation using all 740,000 time-steps for each considered node (260 nodes). Thus, each iteration took about 5 min to perform.

5.2. Stochastic optimization

The K-node is optimized again, considering the stochastic size effect. To show the influence of the parameters on the stochastic size effect, two optimizations have been performed. In the first optimization, a skilled welder/good welding process (welding by robots) has been assumed to weld the structure. A skilled welder/good welding process is capable of welding without considerable scatter (low coefficient of variation, CoV) and will be consistent (high correlation length, b). When welding long and straight welds, it is also common to use robot welding, which can be produced with very high quality. In the second optimization, a bad welding is assumed, where there is a considerable scatter and lesser consistency. This can occur in the case of a less experienced welder or using an unoptimized robotic welding process. The input parameters to the stochastic field in both optimization cases are shown in Table 9. Again, reference damages are required. These are found at intermediate values of the CoV and b, which are also presented in Table 9.

Again 10,000 MC samples are used in the stochastic analysis. The mean stress concentration factor accounting for the statistical size effect in Eq. (17) is considered equal to 1. Using the reference CoV value and correlation length, a total of 7 and 11 kL terms are required to obtain 10% retained information. The longer vertical welds require 11 terms, whereas the shorter horizontal welds require only 7 terms. The welds in the chord are considered to be stochastic and new reference values are calculated for the welds, as the damage is expected to increase compared to the deterministic calculation. In the reference design, a CoV value of 0.1 and a correlation length of 1.2 have been used, which are stated in Table 9. The reference damages are listed in Table 10. The stochastic damages are evaluated as the mean of the maximum damage for each weld for each MC simulation.

The values presented in Table 9, are chosen to demonstrate the difference in stochastic input parameters, as no literature has been found on the CoV and correlation length of stochastic welds. The reference values of CoV = 0.1 and b = 1.2 are used in accordance with the DNV guideline, which assumes a standard deviation of 0.2 on the strength parameter of S–N curves [11]. By using CoV of 0.1 on the stress input, results in a standard deviation of approximately 0.13 on the strength parameter, which is in accordance with the DNV guideline. This is considered reasonable as the standard deviations from S–N curves in the guidelines includes multiple sources of randomness, whereas this investigation only considers the size effect. Again, Eq. (14) is used to determine the stochastic field and Eq. (17) is then used in combination with the strength parameter (CoV) in Table 9 to calculate the stochastic SCF. A sensitivity study has been performed to include the effect of the correlation length and coefficient of variation. The study is presented in Fig. 19 and it shows similar sensitivities for the thickness, width and height as those observed in Fig. 17. The sensitivities for the stochastic input parameters
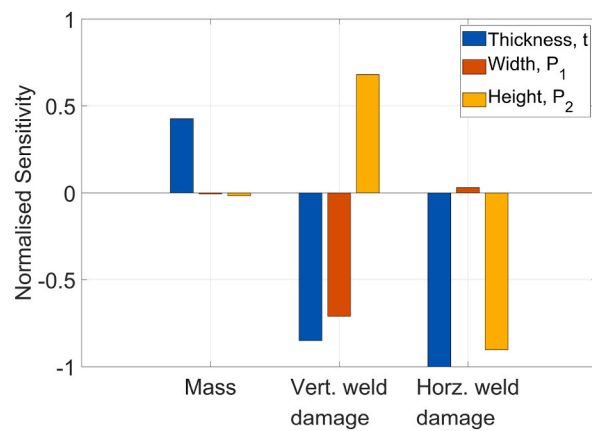
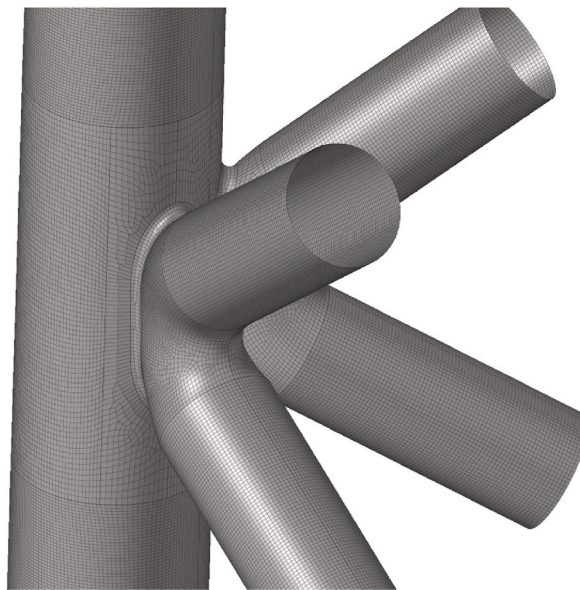**Fig. 17.** Sensitivity study for deterministic optimization of jacket joint.

Fig. 18. Deterministic optimization results with moved weld locations.

Table 8
Optimization results from cast K-node joint using deterministic input parameters.

| Design variable	Original value	Optimized value	Change from original design
Mass (Objective)	1	0.785	−21.5%
t	70 mm	55 mm	−21.4%
P_1	1320 mm	1534 mm	16.2%
P_2	1922 mm	2721 mm	51.6%

Table 9
Optimization parameters used for the stochastic statistical size effect of the welds.

Optimization case	1	2	Reference values
Welding quality	Very good	Poor	Intermediate
CoV	0.05	0.25	0.1
b	5	0.7	1.2

Table 10
Reference equivalent damage for original design considering stochastic fatigue damages at CoV = 0.1 and b = 1.2.

Reference damage	Equivalent damage
$D_{Vertical.ref}$	$1.34x10^{-3}$
$D_{Horizontal.ref}$	$6.23x10^{-4}$
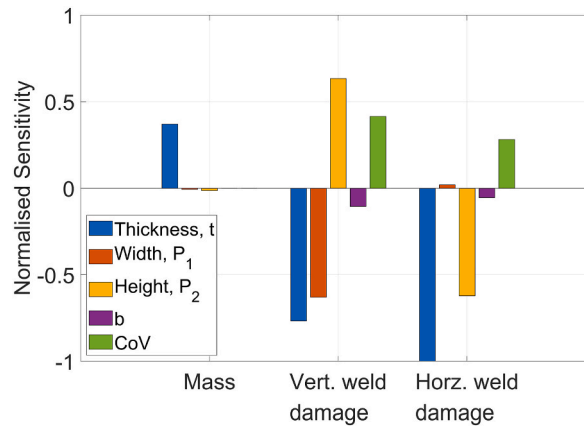
Fig. 19. Sensitivity study for deterministic optimization of jacket joint.

(correlation length and coefficient of variation) show that especially the CoV changes the damage considerably. An increase in CoV increases the damage in the weld. In case of correlation length, it can be seen that an increase in correlation length decreases the damage in the weld. Thus, a more skilled welder or higher quality welding process will decrease the fatigue damage as compared to a less consistent welder.

The optimization, which includes the stochastic size effect is slower than the deterministic optimization. In the case of stochastic analysis, the computation time is approximately 8 h compared to 4 h for the deterministic analysis. This is due to the MC simulations which have been performed for stochastic optimization.

The optimized results are given in Table 11. For case 1 (high quality welds) and case 2 (lower quality welds), it can be clearly seen that using a good welding quality will considerably improve the optimization results. It can also be observed from Table 11, that the values are close to those observed in the deterministic case. However, in the case of a poor-quality weld, a mass reduction of only 2% is achieved. Additionally, it can be seen that the optimization of the poor welds does result in the upper bound values of the width and height (P_1 and P_2) being reached. This is caused by the fact that longer welds are more prone to fatigue damage than shorter welds due to statistical size effect. Increasing the length of the welds to the maximum values will result in lower fatigue life due to the size effect and thus a lesser change of the width and height is observed for the optimization, which consider the lower quality welds.

It can be concluded that the developed optimization framework in combination with the stochastic size effect model can account for welding quality.

The optimization results are highly dependent on the length of the highly stressed area. This was also found by Deinböck et al. [15] in experimentation with different highly stressed weld seam lengths. Similarly, in the present analysis of the K-node structure, it is seen that only a limited length of the weld was exposed to high damages. In the current investigation, the highest fatigue damages are locally very high (up to 10 times higher than the mean damage of the full weld). This means that the effect of correlation length is relatively small, which is also shown in Fig. 19. In this case, as only a few nodes are exposed to high damages, the correlation length has to be extremely large or small to change the results. This can be explained by the fact that only a small portion of the weld is highly loaded. Thus, for failure to happen early in the weld, the defects (modelled using the statistical size effect) should be located at the exact location of high stresses. Instead, the coefficient of variation influences the results as it describes the "magnitude" of the flaws.

Table 11
Optimization results from cast K-node joint using stochastic input parameters.

Design variable	Original value	Optimized value – Good quality weld	Change	Optimized value – Poor quality weld	Change
Mass (Objective)	1	0.798	−20.2%	0.982	−1.8%
t	70 mm	56 mm	−20.0%	61 mm	−13.6%
P_1	1320 mm	1534 mm	16.2%	1521 mm	15.2%
P_2	1922 mm	2721 mm	41.5%	2713 mm	41.2%

With a higher CoV, a larger flaw can be expected. Thus, this will increase the possibility of premature failure in more points of the weld and it is more damaging.

The results from the case studies show that it is possible to optimize a cast node considering the fatigue life of welds. The fatigue life optimization of the cast node results in considerable reduction (up to 20%) in thickness. The optimized performance of cast steel designs has been examined in great detail [2,3,48] and in most of the cases, the fatigue performance of the cast joints is observed to be better than the traditional welded joints. In the publications by Haldimann-Sturm and Nussbaumer [3] and Nussbaumer et al. [48], cast steel joints were similarly investigated and found to perform better than traditional welded joints. However, in Ref. [48], the results showed that fatigue failure was still governing for the design, but the actual failure location was moved. Instead of the fatigue failure occurring at the cast part, fatigue failure occurred at the girth butt welds at the casting stubs. This shows the necessity of evaluating the fatigue performance of welds in cast steel designs. The use of cast steel solutions, however, also requires other types of considerations such as the production of the cast steel joints because it can be difficult and requires special consideration. The proposed optimization framework can be further extended to include the cast steel production requirements and base material fatigue. Base material fatigue refers to the fatigue life of the non-welded cast steel, which has been shown to be highly influenced by defects in the cast material [11,49,50]. This must be considered when replacing traditional rolled steel with cast steel. This has not been considered in the presented work. There is also a large variability of weld geometry, which has not been considered in the present work. This variability can be included in the proposed framework by using the KL expansion.

6. Conclusions

In this work, a framework has been developed for optimization of welded structures considering the fatigue damage of welds. The framework is easy to implement and it can be used for many types of welded structures, as the framework utilizes the finite-difference approach for gradient estimation.

The proposed optimization framework can incorporate the statistical size effect. The size effect is modelled using a stochastic expression of an additional stress concentration factor, which can be added to the deterministic stresses calculated in a FE analysis. The Karhunen-Loéve expansion is used to model the effect of longer welds, which are more prone to fatigue damage.

Two case studies are presented in this paper. In the first case study, a simple plate structure is considered to validate the optimization framework and stochastic size effect. The results of the simple plate structure show that the optimization framework can be used to optimize the weld orientation and provide robust statistical results. In the second case study, a full-scale K-node is optimized considering the mass of a cast steel joint, including the effects of high-quality welding or low-quality welding, which are stochastically modelled. The results have shown that the proposed optimization framework can be used with confidence, when considering the stochastic size effect for welded joints.

Declaration of competing interest

The authors declare that they have no known competing financial interests or personal relationships that could have appeared to influence the work reported in this paper.

Acknowledgements

References

[1] Wirsching PH. Fatigue reliability for offshore structures. J Struct Eng 1984;110:2340–56.
[2] Wang L, Jin H, Dong H, Li J. Balance fatigue design of cast steel nodes in tubular steel structures. Sci World J 2013;2013:1–10.
[3] Haldimann-Sturm SC, Nussbaumer A. Fatigue design of cast steel nodes in tubular bridge structures. Int J Fatig 2008;30:528–37.
[4] Oest J, Sørensen R, Overgaard LC, Lund E. Structural optimization with fatigue and ultimate limit constraints of jacket structures for large offshore wind turbines. Struct Multidiscip Optim 2017;55:779–93.
[5] Oest J, Lund E. Topology optimization with finite-life fatigue constraints. Struct Multidiscip Optim 2017;56:1045–59.
[6] Suresh S, Lindström SB, Thore C-J, Torstenfelt B, Klarbring A. Topology optimization using a continuous-time high-cycle fatigue model. Struct Multidiscip Optim 2019;61:1011–25.
[7] Motlagh AA, Shabakhty N, Kaveh A. Design optimization of jacket offshore platform considering fatigue damage using Genetic Algorithm. Ocean Eng 2021;227:108869.
[8] Chew K-H, Tai K, Ng EYK, Muskulus M. Analytical gradient-based optimization of offshore wind turbine substructures under fatigue and extreme loads. Mar Struct 2016;47:23–41.
[9] Wöhler A. Versuche zur Ermittlung der auf die Eisenbahnwagenachsen einwirkenden Krafte und die Widerstandsfahigkeit der Wagen-Achsen (In English: experiments to determine the forces acting on the railroad car axles and the resistance of the car axles). Zeitschrift für Bauwesen 1860;10:583–614.
[10] Hobbacher AF. Recommendations for fatigue design of welded joints and components. Springer International Publishing; 2016.
[11] DNV-GL. DNVGL-RP-C203 - fatigue design of offshore structures. DNVGL; 2019.
[12] DS/EN. Eurocode 3: design of steel structures - part 1-9: fatigue. Danish Standards; 2007.
[13] Fricke W, Müller-Schmerl A. Uncertainty modeling for fatigue strength assessment of welded structures. J Offshore Mech Arctic Eng 1998;120:97–102.
[14] Pedersen MM. Thickness effect in fatigue of welded butt joints: a review of experimental works. Int J Steel Struct 2019;19:1930–8.

[15] Deinböck A, Hesse A-C, Wächter M, Hensel J, Esderts A, Dilger K. Increased accuracy of calculated fatigue resistance of welds through consideration of the statistical size effect within the notch stress concept. Weld World 2020;64:1725–36.
[16] Ghanem RG, Spanos PD. Stochastic finite elements: a spectral approach. New York: Springer; 1991.
[17] Stefanou G. The stochastic finite element method: past, present and future. Comput Methods Appl Mech Eng 2009;198:1031–51.
[18] Aldosary M, Wang J, Li C. Structural reliability and stochastic finite element methods. Eng Comput 2018;35:2165–214.
[19] Arregui-Mena Je, David Margetts L, Mummery PM. Practical application of the stochastic finite element method. Arch Comput Methods Eng 2014;23:171–90.
[20] Guo T, Frangopol DM, Chen Y. Fatigue reliability assessment of steel bridge details integrating weigh-in-motion data and probabilistic finite element analysis. Comput Struct 2012;112–113:245–57.
[21] Peng XQ, Geng L, Liyan W, Liu GR, Lam KY. A stochastic finite element method for fatigue reliability analysis of gear teeth subjected to bending. Comput Mech 1998;21:253–61.
[22] Larsen MLo, venskjold, Arora V, Lützen M, Pedersen RR, Putnam E. Fatigue life estimation of the weld joint in K-node of the offshore jacket structure using stochastic finite element analysis. Mar Struct 2021;78:103020.
[23] Larsen ML, Arora V, Clausen HB. Finite element shape optimization of weld orientation in simple plate structure considering different fatigue estimation methods. Proc Struct Integrity 2021;31:70–4.
[24] Sines G. Failure of materials under combined repeated stresses with superimposed static stresses. NACA TN 3495. NACA; 1955.
[25] Darrell S, Marquis GB. Multiaxial fatigue. PA: SAE International: Warrendale; 2000.
[26] Gough HJ, Pollard HV. The strength of metals under combined alternating stresses. Proc Inst Mech Eng 1935;1:1–101.
[27] ASTM. E1049-85: standard practices for cycle counting in fatigue analysis. 2017.
[28] DVS. DVS Merkblatt 0905: industrielle Anwendung des Kerbspannungskonzeptes für den Ermüdungsfestigkeitsnachweis von Schweißverbindungen, In English: industrial application of the notch stress approach for the fatigue assessment of welded joints; 2017.
[29] ANSYS Inc. ANSYS workbench 2020 R2. 2020.
[30] Simulia. Abaqus. https://www.3ds.com/products-services/simulia/products/abaqus/; 2021. 2021.
[31] HyperWorks. Altair HyperWorks software. 2019.
[32] Lotsberg I. Assessment of the size effect for use in design standards for fatigue analysis. Int J Fatig 2014;66:86–100.
[33] Overbeeke JL, Wildschut H. The influence of plate thickness on the endurance of welded joints. In: Noordhoek C, Back J, editors. Proceedings of the 3rd international ECSC offshore conference on steel in marine structures (SIMS '87). Delft, The Netherlands: Elsevier; 1987.
[34] Karhunen K. Ueber lineare methoden in der Wahrscheinlichkeitsrechnung. In: In English: on linear methods in probability and statistics; 1947.
[35] Papadopoulos V, Giovanis DG. Stochastic finite element methods. Springer International Publishing; 2018.
[36] Papoulis A. Probability, random variables and stochastic processes. Mcgraw-Hill College; 1991.
[37] Rahman S. A Galerkin isogeometric method for Karhunen}Loeve approximation of random fields. Comput Methods Appl Mech Eng 2018;338:533–61.
[38] Betz W, Papaioannou I, Straub D. Numerical methods for the discretization of random fields by means of the Karhunen-Loéve expansion. Comput Methods Appl Mech Eng 2014;271:109–29.
[39] Spanos PD, Beer M, Red-Horse J, Karhunen. Loeve expansion of stochastic processes with a modified exponential covariance kernel. J Eng Mech 2007;133:773–9.
[40] Adhikari S, Friswell MI. Distributed parameter model updating using the Karhunen Loeve expansion. Mech Syst Signal Process 2010;24:326–39.
[41] Larsen ML, Adhikari S, Arora V. Analysis of stochastically parameterized prestressed beams and frames 2021;249:113312.
[42] Liu Y, Mahadevan S. Efficient methods for time-dependent fatigue reliability analysis. AIAA J 2009;47:494–504.
[43] Liu Y, Mahadevan S. Stochastic fatigue damage modeling under variable amplitude loading. Int J Fatig 2007;29:1149–61.
[44] Miner MA. Cumulative damage in fatigue. J Appl Mech 1945;12:A159–64.
[45] Altair engineering inc. Altair HyperStudy 2019 - user guide. 2019.
[46] DNV-GL. DNVGL-ST-0126 - support structures for wind turbines. DNVGL; 2018.
[47] DNV-GL. DNVGL-ST-0437 - loads and site conditions for wind turbines. DNVGL; 2016.
[48] Nussbaumer A, Haldimann-Sturm S, Schumacher A. Fatigue of bridge joints using welded tubes or cast steel node solutions. In: Proceedings of the 11th international symposium and IIW international conference on tubular structures. Canada: Quebec City; 2006. p. 56–63.
[49] Sigl KM, Hardin RA, Stephens RI, Beckermann C. Fatigue of 8630 cast steel in the presence of porosity 2004;17:130–46.
[50] Hardin RA, Beckermann C. Prediction of the fatigue life of cast steel containing shrinkage porosity 2009;40:581–97.